CHAPTER V

DENDRITIC POLYANILINE NANOPARTICLES SYNTHESIZED BY CARBOXYMETHYL CHITIN TEMPLATING

5.1 Abstract

Dendritic polyaniline (PANI) nanoparticles were synthesized via oxidative polymerization of aniline, using ammoniumperoxodisulfate as an oxidant, and CM-chitin as a template. The reaction was performed under acidic conditions and the template was removed after the polymerization was completed. Molecular characterization (including UV-vis, FTIR, TGA, and XRD) suggests that the structure of the synthesized dendritic PANI nanoparticles is identical to that of the emeraldine form of PANI, synthesized by the conventional route (without the addition of the CM-chitin template). SEM images reveal that the dendritic PANI nanoparticles have an average diameter in the nanometer range, and are globular in shape, with radially oriented PANI dendrites; in contrast, irregularly-shaped aggregates of PANI are obtained using the conventional synthesis. It was further found that the size of the dendritic PANI nanoparticles is dependent on the CM-chitin content. The higher the CM-chitin concentration, the smaller is the size of the dendritic PANI nanoparticles obtained. An interpretation of these observations and a possible formation mechanism are proposed based on self-assembly between the CM-chitin chains and the aniline monomer.

5.2 Introduction

Polyaniline (PANI) is one of the most extensively studied conductive polymers, due to its ease of synthesis by chemical or electrochemical polymerization, facile control of electrical conductivity, good environmental stability, and economic production, due to the inexpensive monomer (Cho *et al.* 2004; Zhang, *et al.* 2006; Cheng *et al.* 2005). It is well established that PANI can be transformed into a conducting state, the emeraldine *salt* form (PANI ES), via a doping process with acids such as HCl, and can be converted to an insulating state, the emeraldine *base*

form (PANI EB), by treatment with bases such as NH_4OH or $NaOH$, referred to as the dedoping process (Pinto, Carrion, Ayala, Ortiz-Marciale 2005). This versatility has made polyaniline attractive for numerous applications, including sensors (Ma, Wang, Li, Chen, Bai 2006: Xing et al. 2006), batteries (Wang, Mottaghitalab, Too, Spinks, Wallace 2007), electrodes (Ghanbari, Mousavi MF, Shamsipur 2007), display devices (Shah, Holze 2006), anticorrosion coatings (Sazou, Kourouzidou, Pavlidou 2007), and field effect transistors (Xing, Zhao, Niu, Wu, Wang, Wang 2006). Recently, the creation of PANI nanostructures has become of particular interest to the physics communities for potential application in nanoelectronic devices and molecular sensors, due to their extremely high surface area, synthetic versatility, and low cost (He et al. 2005). To synthesize PANI nanostructures with different morphologies including tubes, rods, fibers, and spheres, diverse methods such as template (Xiong et al. 2004), template-free (Cheng et al. 2005), electrospinning (Li et al. 2006), seeding (Zhang et al. 2004, Zhang and Manohar 2004), and interfacial polymerization (Huang, Kaner 2004; Sawall, Villahermosa, Lipeles, Hopkins 2004) have been explored. In addition to such morphologies, a dendritic PANI structure would seem to be of interest, because it creates a large surface area and more functional sites, which is important for sensor applications (Yan, Han, Yang, Tay 2007) or drug delivery systems (Low, Seetharaman, He, Madou 2000). Previously, Li et al. reported the synthesis of a dendritic PANI particle, with a diameter of 20-25 micrometers, consisting of radially aligned PANI nanotubes, obtained using tartaric acid as a dopant and ammoniumperoxodisulfate (APS) as an oxidizing agent under static conditions (Li, Pang, Xie, Wang, Peng, Zhang 2006). The formation mechanism is presumed to proceed via the self-assembly process of dopant or dopant/aniline salt. However, although composed of PANI nanotubes, the overall sizes of the synthesized dendritic PANI particles obtained in this previous work were relative large, in the range of several micrometers, and a non-uniform morphology was obtained. In the present study, we present a simple method to synthesize dendritic PANI nanoparticles which are more uniform in size and have an average diameter in the nanometer range, using carboxymethyl chitin (CM-chitin) as a structure-directing molecule or template.

CM-chitin is a water soluble derivative of chitin obtained via the carboxymethylation of chitin with monochloroacetic acid under basic conditions. CM-chitin can self-assemble and exhibits an emulsifying property under acidic conditions, which is the condition for PANI synthesis, due to their amphiphilic structure (Ueno, Yokota, Kitaoka, Wariishi 2007), consisting of the equatorial hydrophilic groups (including -OH, $-NH_3^+$, $-NH-COCH_3$, and $-OCH_2COOH$), which act as the hydrophilic shell, and the axial hydrophobic planes, which act as the hydrophobic core. The hydrophobic core serves as the reaction template for monomer accumulation and subsequent polymerization when the oxidant is added. Owing to the solubility of CM-chitin in water, the CM-chitin template, moreover, is easily removed by washing with water to obtain a pristine dendritic PANI product after the polymerization of aniline is complete. A mechanism for formation of the dendritic PANI nanoparticles is proposed, based on a self-assembly process, and the effect of CM-chitin content on the morphology of the dendritic PANI nanoparticles is investigated.

5.3 Experimental

5.3.1 Materials

Aniline monomer was purchased from Merck. and was distilled under reduced pressure prior to use. AR grade ammoniumperoxodisulfate (APS) was also purchased from Merck.

Chitin, with a degree of deacetylation (%DD) equal to 20%, measured by the method of Baxter *et al.* (Baxter, Dillon, Taylor 1992), was prepared from shrimp shell (*Penaeus merguiensis*), kindly supplied by Surapon Food Co. Ltd, Thailand. AR grade hydrochloric acid, sodium hydroxide, monochloroacetic acid, and acetone were purchased from Labscan and used as received.

5.3.2 Preparation of Carboxymethyl Chitin (CM-chitin)

CM-chitin, with a degree of substitution (DS) equal to 0.43, was prepared by the reaction of chitin powder with monochloroacetic acid under basic conditions according to the method described by Wongpanit *et al.* (Wongpanit *et al.*

2005). In a typical procedure, CM-chitin was prepared by suspending 5 g of chitin powder in 100 g of 42 %w/w NaOH. The suspension was stored under reduced pressure for 30 min. Then, 160 g of crushed ice was added to the suspension and the mixture was stirred at below 5°C for 30 min. A pre-cooled solution at a temperature below 5°C, containing 27 g monochloroacetic acid in 70 ml of 14% w/w NaOH, was slowly added to the mixture with vigorous stirring. The reaction was maintained at 0-5°C for 30 min. After settling at room temperature overnight, the mixture was neutralized with glacial acetic acid and subsequently dialyzed in running water, followed by dialysis with distilled water for 1 day. The dialysate was centrifuged at 10,000 rpm for 20 min to remove the insoluble material. A white solid was recovered from the supernatant by adding it drop-wise into acetone. The product was washed with ethanol, filtered, and dried in a vacuum at room temperature.

5.3.3 Synthesis of Dendritic Polyaniline Nanoparticles

Dendritic PANI nanoparticles were synthesized in aqueous solution by the oxidative polymerization of aniline, using APS as an oxidant, in the presence of CM-chitin, acting as a template. The synthesis procedure is described as follows: 8 g (0.086 mol) of aniline was poured into 50 g of aqueous CM-chitin solutions (at concentrations of 0.5 wt%, 1 wt%, and 2 wt%) and the mixture was cooled to 0°C with mechanical stirring at 300 rpm for 1 h. 100 ml of 1.5-M HCl was added drop-wise into the mixture within 30 min and the solution was maintained with mechanical stirring for 30 min. Next, a pre-cooled solution, at a temperature below 5°C, containing 10 g (0.048 mole) APS in 100 ml of 1.5-M HCl was added drop-wise within 30 min, and the reaction was stirred at 0°C for 4 h to complete the polymerization. The suspension was then centrifuged at 11,000 rpm for 20 min and the precipitated product was subjected to dialysis with an excess amount of distilled water, until becoming neutral. Finally, the precipitated product was filtered, washed with distilled water, dried under reduced pressure for 2 days, and kept in desiccators prior to use.

5.3.4 Characterization

UV-visible spectra were obtained with a Shimadzu UV-VIS spectrometer, model 2550, in the wavelength range 200-900 nm.

FTIR spectra were recorded using a Thermo Nicolet Nexus 670 FTIR spectrometer in the absorbance mode at 32 scans with a resolution of 4 cm^{-1}. Spectra in the frequency range of 4,000-400 cm^{-1} were measured using a deuterated triglycerinesulfate detector with a specific detectivity of 1 × 10^9 cm·Hz$^{1/2}$·w^{-1}.

The morphologies of the polyaniline nanoparticles were investigated using a scanning electron microscope (JOEL, model JSM-5800LV) at 15 kV. Samples were prepared by the dispersion of polyaniline in distilled water, and placing a drop onto a brass stub before gold sputtering.

Thermogravimetric analysis was performed using a DuPont Instrument TGA 5.1, model 2950, in the temperature range 30-800°C at a heating rate of 10°C/min under a nitrogen atmosphere.

X-ray diffraction (using a Rigaku, model D/MAX-2000) was carried out in continuous mode with a scan speed of 5°/min, covering angles 2θ between 5 and 50°. Cu Kα_1 radiation was used as the X-ray source.

The electrical conductivity was measured at 25°C using a custom-made two-point probe with an electrometer/ high resistance meter (Keithley, model 7517A).

5.4 Results and Discussions

5.4.1 UV-visible Spectra

UV-vis spectra were used to investigate the electronic states of PANI synthesized using a CM-chitin template, in both the emeraldine salt (PANI ES) and emeraldine base (PANI EB) forms. PANI was dispersed in 1.5-M HCl to form PANI ES, and dispersed in N-methyl-2-pyrollidone (NMP) to allow dedoping to PANI EB (Yuan, Kuramoto, Su 2002). The PANI ES showed absorption peaks at 410 and 810 nm, attributed to the presence of cation radicals (polarons) and the formation of bipolarons, respectively (Xian et al. 2007). This confirms the doped state of PANI ES. In contrast, the absorption peaks of the soluble part of PANI EB in NMP were observed at approximately 320 and 620 nm, assigned to the π-π* transition of the

benzenoid ring and the exciton absorption of the quinoid ring, respectively (He *et al.* 2005). Additionally, the integral area under these two peaks quantified the concentration of the imine and the amine structural units as expected from the emeraldine oxidation states of PANI (Yang *et al.* 2003). The UV-vis spectra of PANI synthesized using the CM-chitin template in both PANI ES and PANI EB forms were identical to those of PANI synthesized by the conventional method (without the addition of the CM-chitin template).
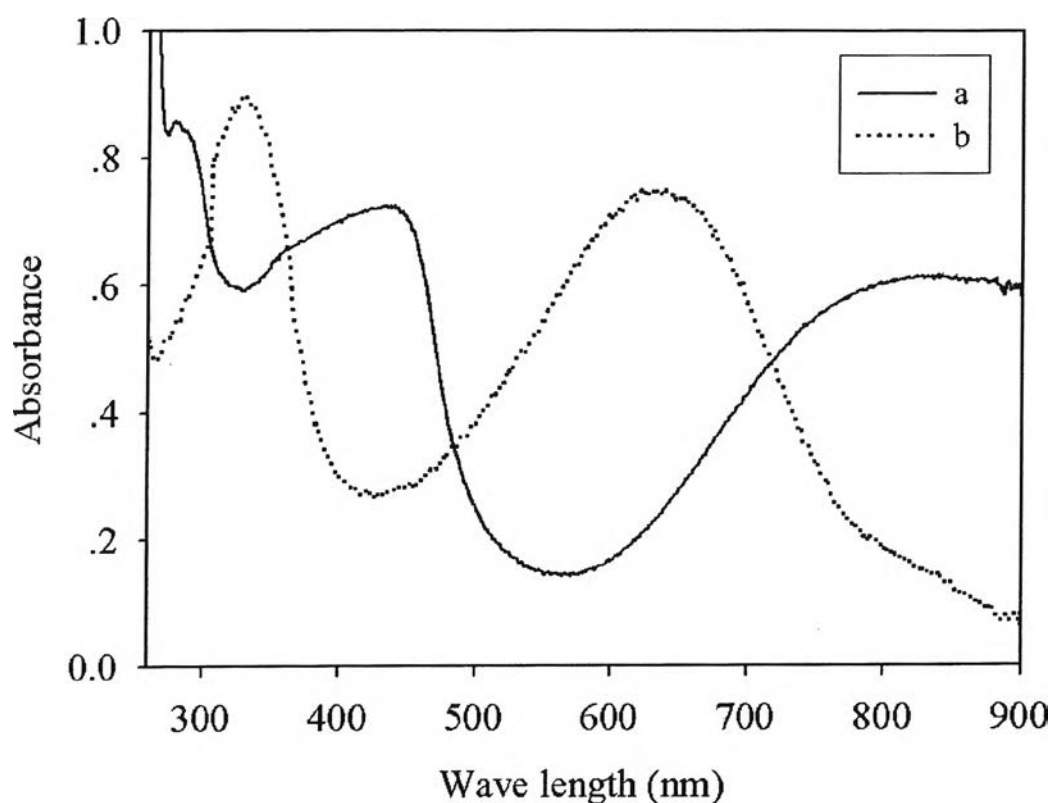
Figure 5.1 UV-visible spectra of the synthesized PANI nanoparticles: a) emeraldine salt form (PANI ES) and b) emeraldine base form (PANI EB).

5.4.2 Morphology and Formation Mechanism

Scanning electron microscopy (SEM) was used to investigate the morphology of the synthesized dendritic PANI nanoparticles obtained by the CM-chitin template. As shown in figure 5.2a, the SEM image revealed globular PANI nanoparticles, with diameters in the nanometer range, whose surfaces are covered

with radially aligned PANI dendrites. In contrast, irregularly-shaped PANI aggregates were observed in the PANI synthesized by the conventional method, as shown in figure 5.2b. A possible formation mechanism may be proposed, based on a self-assembly process involving CM-chitin and aniline monomer. Experimentally, aniline monomer is first suspended in the CM-chitin solution with agitation. When 1.5-M HCl is added into the solution (the pH of the mixture solution decreases below 1), most aniline monomers are transformed into amphiphilic anilinium ions, the protonated aniline monomer (Jang, Bae, Lee 2005). A clear solution is obtained in the reaction mixture since the protonated CM-chitin and the anilinium ion are both soluble. To gain further insight into the role of the CM-chitin in the dispersion of aniline monomer, analogous experiments were performed, using toluene instead of the aniline monomer. After adding 1.5-M HCl to a suspension of toluene in CM-chitin solution, followed by agitating the mixture for 1 h, it was found that a stable dispersion of toluene persisted for several hours, whereas phase separation occurred rapidly (1-2 min) when no CM-chitin was present. This confirms a significant emulsifying property of protonated CM-chitin on aqueous toluene mixtures. Such an emulsifying phenomenon can be explained in terms of the amphiphilic character of the CM-chitin functional groups, when the pH of the dispersion is lowered below 1); under such conditions, the protonation of high polarity carboxymethylate ions (-OCH_2COO^-) to the lower polarity acid form (-OCH_2COOH) occurs, while, in contrast, the low polarity amino groups convert to higher polarity protonated forms (-NH_3^+). Ueno et al. (Ueno et al. 2005) reported that polysaccharides such as CM-chitin, which have equatorially-substituted glucopyranose rings, exhibit amphiphilic character, with equatorial hydrophilic edges, and axial hydrophobic planes. Therefore, the protonated CM-chitin molecules can form core-shell structures in aqueous solution where the equatorial hydrophilic groups (including -OH, -NH_3^+, -NH-$COCH_3$, and -OCH_2COOH) orient toward the exterior aqueous phase to form the hydrophilic shell while the axial hydrophobic planes (-CH_2- bond) orient towards the interior to form the hydrophobic core. The hydrophobic core can solubilize the hydrophobic part of the aniline molecules by forming a strong interaction with the sp^2 hybridized orbital of aromatic rings via CH-π bonding (Palma, Himmel, Brady 2000), and thus function as a reaction template for monomer accumulation (Sahiner

2007). The anilinium ion can migrate into the core-shell structure, oriented radially with the benzene ring towards the hydrophobic core and the ammonium group towards the polar shell, and subsequently form a nucleating site at the interface of the core-shell structure by electrostatic interaction between the chloride anions of the HCl-doped quinoid imine and the ammonium group of CM-chitin, as well as H-bonding interaction between the benzenoid amine and H_2O coexisting in the PANI doped with HCl (Jang *et al.* 2005). Through the addition of APS, used as the oxidant, the polymerization of the anilinium ion occurs radially from the nucleating site in the template, which provides a local environment to promote the *para*-substitution or head-to-tail coupling of the anilinium ion radical (Cruz-Silva, Romero-Garcia, Angulo-Sanchez, Ledezma-Perez, Arias-Matin, Moggio, Flore-Loyola 2005), and hence generate the radially aligned dendritic PANI structure, as shown in schematic 5.1.
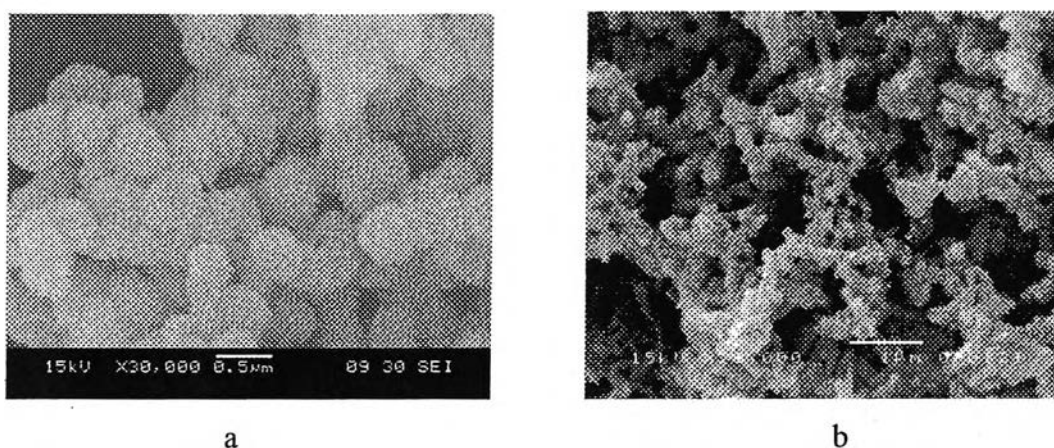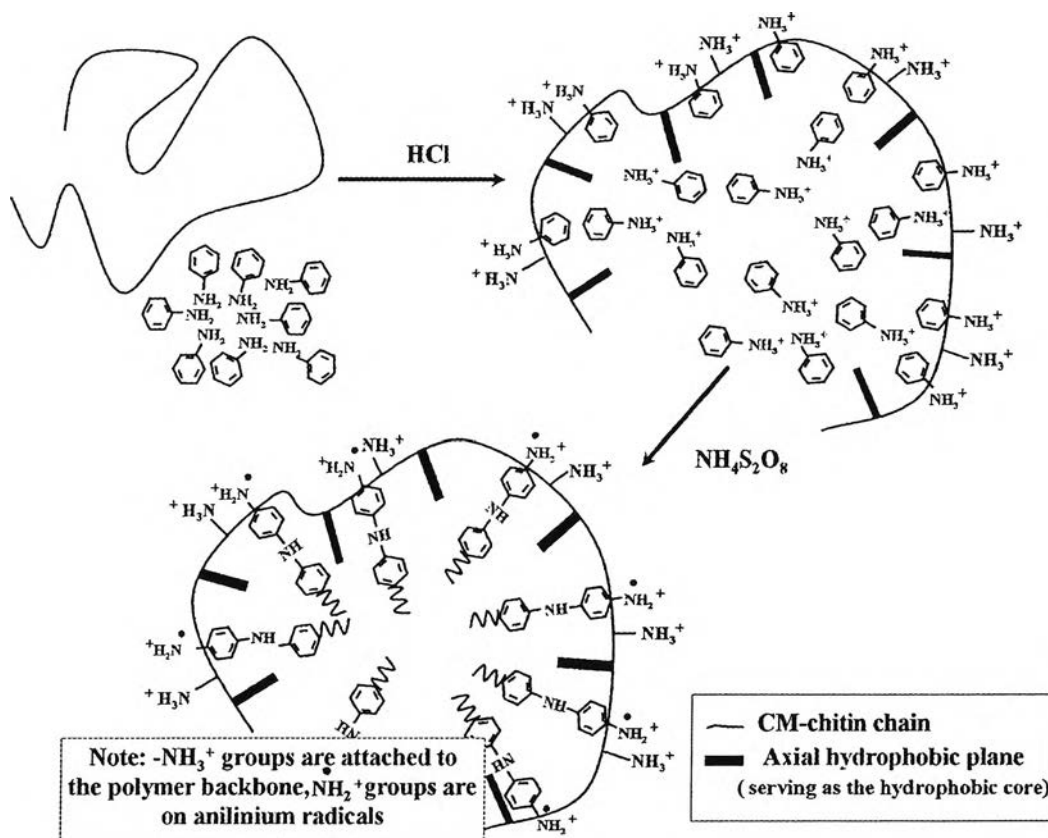

a   b

Figure 5.2 SEM images of polyaniline nanoparticle: a) dendritic PANI nanoparticle; b) conventional PANI.

Figure 5.3 shows the SEM images of the synthesized dendritic PANI nanoparticles with and without the removal of the CM-chitin template. It was determined that the dendritic PANI nanoparticles grow inside the CM-chitin template at an early state (see Fig. 5.3c), and subsequently separate out from CM-chitin template when there is increasing hydrophobicity, due to the extent of polymerization, which overcomes the hydrophilic interaction between the aniline oligomers and the CM-chitin template. Moreover, it was also found that the

concentration of added CM-chitin plays an important role in determining the diameter of the synthesized dendritic PANI nanoparticles. The average diameter (based on a sample of n = 50 particles) of dendritic PANI nanoparticles decreased, at fixed aniline content (0.086 mole of aniline), from 485 ± 40 to 392 ± 34 and 340 ± 23 nm when the CM-chitin concentration was increased from 0.5 wt% (0.5CM-chitin) to 1 wt% (1CM-chitin) and 2 wt% (2CM-chitin), respectively (Fig. 5.3b, 5.3d, and 5.3f). This result seems reasonable, because increased concentration of the CM-chitin template increases the number of nucleating sites (Stejkal, Sapurina 2004). Since a higher number of nucleating sites leads to a lower amount of monomer uptake in each hydrophobic core, the result is a decrease in size of the dendritic PANI nanoparticles. Additionally, upon investigation of the nanoparticle size distribution, it was found that the use of the CM-chitin template results in formation of highly uniform dendritic PANI nanoparticles with a narrow size distribution (see the insets to Figure 5.3). This suggests that the self-assembled CM-chitin template provides rather well-defined spaces for accumulation of the aniline monomer and subsequent polymerization.

Schematic 5.1 Proposed formation mechanism of dendritic polyaniline nanoparticles using CM-chitin template. Note, not shown in the diagram are the chloride counterions and associated water of asolvation which accompany the clustering of anilinium ions.
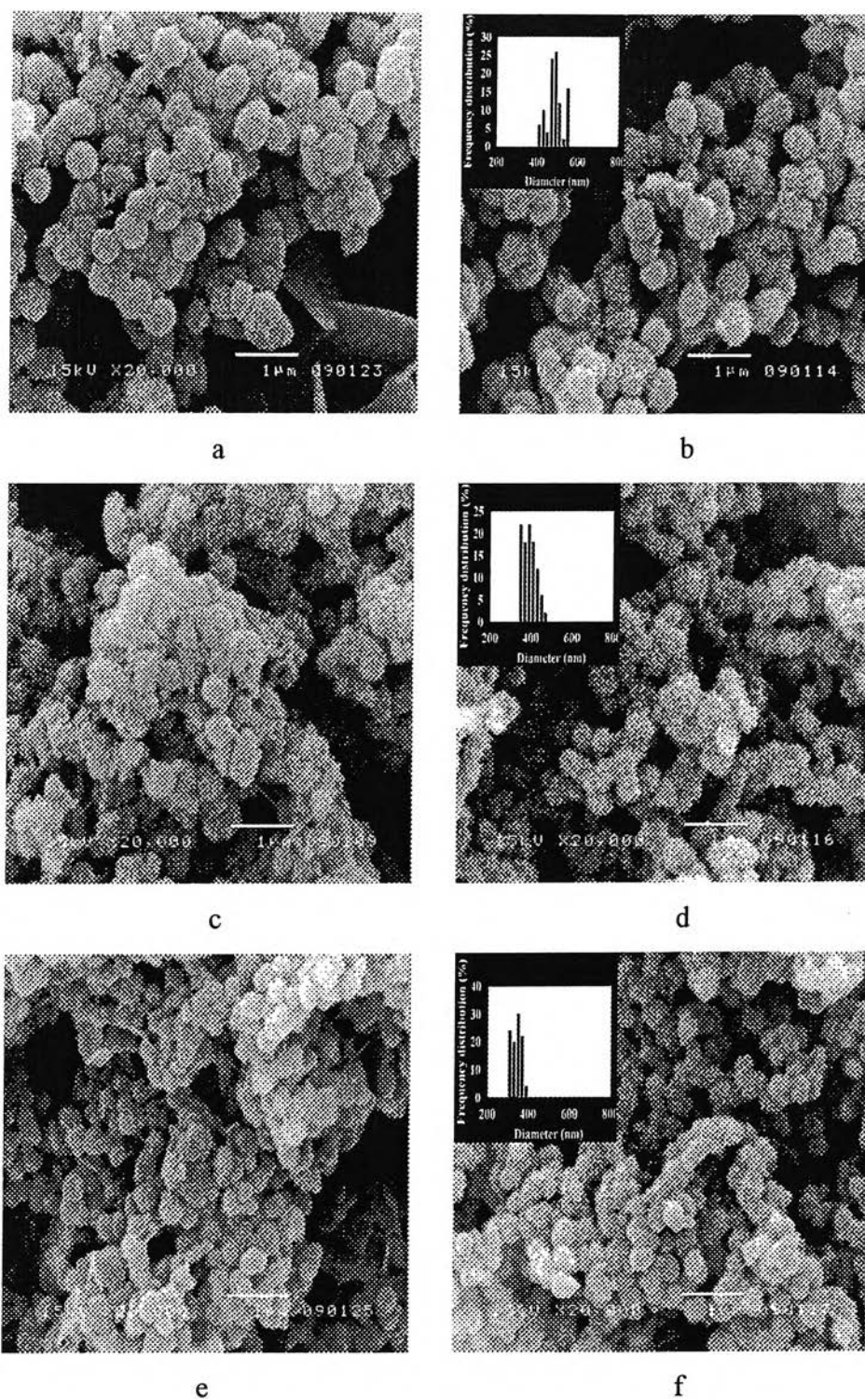
Figure 5.3 SEM images of polyaniline nanoparticle obtained from different CM-chitin concentrations: a) PANI-(0.5CMCT) without washing; b) PANI-(0.5CMCT) washed with H_2O; c) PANI-(1CMCT) without washing; d) PANI-(1CMCT) washed with H_2O; e) PANI-(2CMCT) without washing; f) PANI-(2CMCT) washed with H_2O.

5.4.3 FTIR Spectra

The chemical structure of the synthesized dendritic PANI nanoparticles was identified by FTIR spectra, as shown in figure 5.4. Figure 5.4a presents the FTIR spectrum of PANI synthesized by the conventional method. Characteristic peaks appear at 1565, 1482, 1293, 1100, and 789 cm^{-1} assigned to C=C stretching of the quinoid ring, C=C stretching of the benzenoid ring, C-N stretching, N=Q=N stretching (Q representing the quinoid ring), and out-of-plane deformation of C-H in the 1, 4-disubstituted benzene ring, respectively (He *et al.* 2005; Li *et al.* 2006; Bai *et al.* 2006). In contrast, as shown in figure 5.4e, the characteristic peaks of CM-chitin in the acid form arise at 1743, 1650, 1379, and 1067 cm^{-1} corresponding to COOH stretching, asymmetric and symmetric C=O stretching, and C-O-C stretching of the pyranose ring, respectively (Mi, Chen, Tseng, Kuan, Shyu 2006). With regard to the dendritic PANI nanoparticles formed in the presence of 0.5 wt% CM-chitin template, no significant difference was found in the FTIR spectra of the synthesized dendritic PANI nanoparticles (Fig. 5.4b-5.4c) compared to the conventional PANI. This confirms the complete removal of the CM-chitin template. However, a weak peak at 1726 cm^{-1}, assigned to COOH stretching, was observed in spectrum of dendritic nanoparticles formed in the presence of 2 wt% CM-chitin concentration (Fig. 5.4d). This result suggests incomplete removal of the CM-chitin template at the higher CM-chitin concentration.
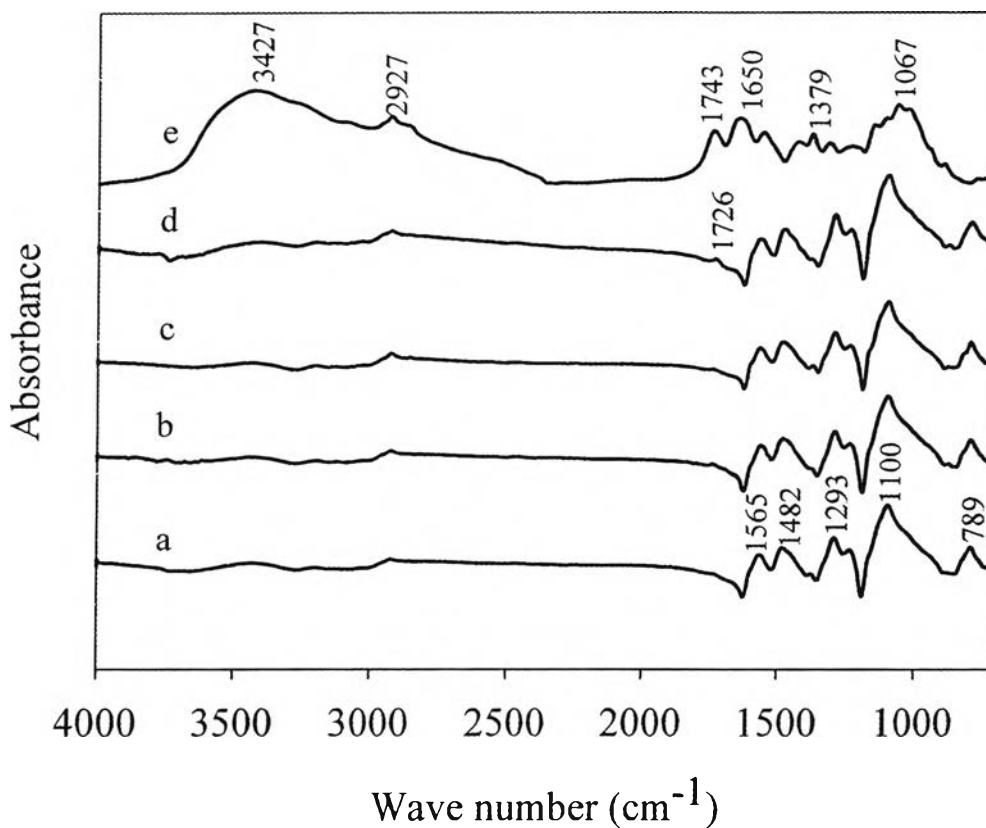
Figure 5.4 FTIR spectra of polyaniline nanoparticle: a) conventional PANI; b) PANI-(0.5CMCT); c) PANI-(1CMCT); d) PANI-(2CMCT); e) CM-chitin (acid form).

5.4.4 Thermogravimetric Analysis (TGA)

Figure 5.5 shows the TGA thermograms of the dendritic PANI nanoparticles, synthesized using different CM-chitin concentrations. The CM-chitin template exhibits two discrete weight losses at approximately 80 and 283°C corresponding to the loss of water and the degradation of CM-chitin chains, respectively, as shown in figure 5.5a. In contrast, three discrete weight losses, occurring at approximately 80, 280, and 500°C, were observed in all samples of the synthesized PANI. These weight losses were due to the loss of water, the elimination of the dopant, and the degradation of the PANI chains, respectively (Kan *et al.* 2006; Chan *et al.* 1989; Neoh *et al.* 1990). However, under the same drying conditions, the dendritic PANI nanoparticles (Fig. 5.5b-5.5c) showed a higher water affinity than

that of conventional PANI (Fig. 5.5d). This can likely be attributed to the high surface area of the dendritic PANI nanoparticles, which can interact with larger amounts of water compared to conventional PANI.
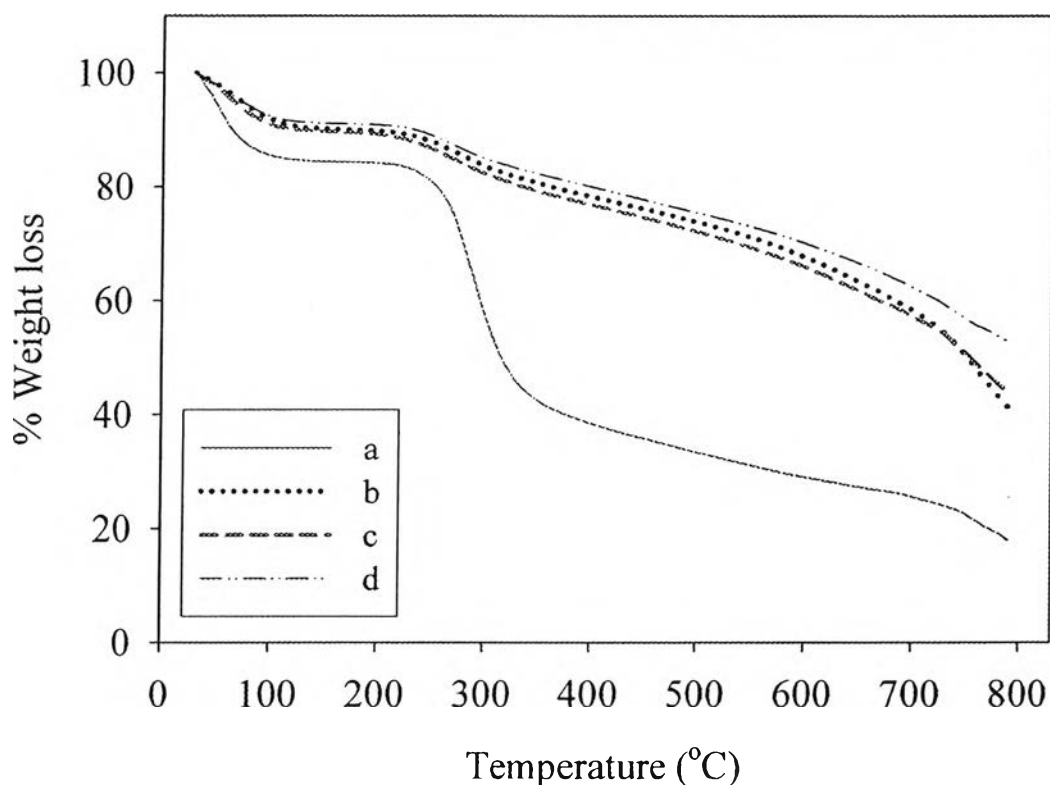

Figure 5.5 TGA thermograms of polyaniline nanoparticle: a) CM-chitin powder; b) PANI-(1CMCT); c) PANI-(2CMCT); d) conventional PANI.

5.4.5 Wide angle X-ray Diffraction (WAXD)

It is important to confirm the presence of the crystalline structure of PANI which endows a high electrical conductivity (Xiong, *et al.* 2004). The X-ray diffraction patterns of CM-chitin and the synthesized dendritic PANI are presented in figure 5.6. CM-chitin exhibits a weak diffraction peak at $2\theta = 9°$ and a broad diffraction peak centered at $2\theta = 20°$, suggesting primarily an amorphous structure (Fig. 5.6d) (Maramutsu, Masuda, Yoshihara, Fujisawa 2003). For the conventional PANI ES (Fig. 5.6a), six main diffraction peaks in the range of $2\theta = 9\text{-}30°$ are evident. This result is consistent with the known partially-crystalline structure of

PANI ES (Xing *et al.* 2006; Li *et al.* 2007). The dendritic PANI ES nanoparticles, synthesized using the CM-chitin template, showed (Fig. 5.6b-5.6c) identical diffraction peaks to the conventional PANI ES. This indicates that the addition of CM-chitin as a template causse a change in morphology, but does not alter the crystalline structure of the resulting dendritic PANI.
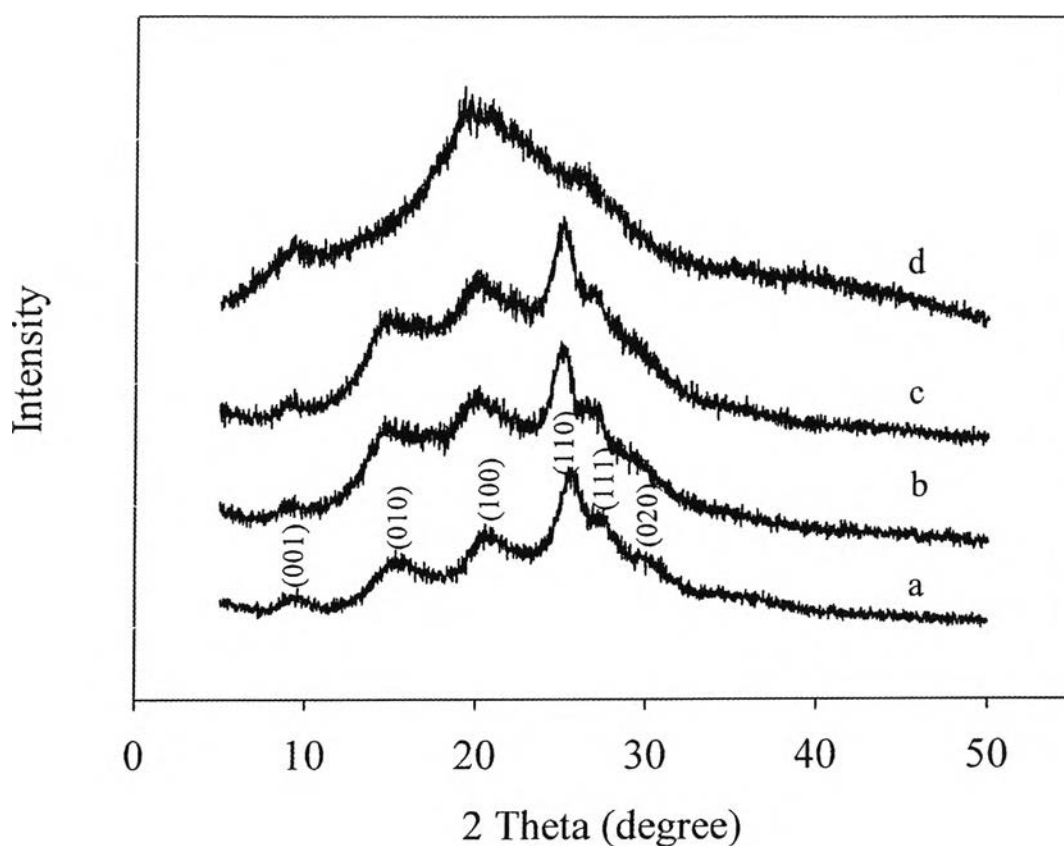

Figure 5.6 XRD patterns of polyaniline nanoparticle: a) conventional PANI; b) PANI-(0.5CMCT); c) PANI-(2CMCT); d) CM-chitin powder.

5.4.6 Electrical Property

The electrical conductivities of all synthesized PANI samples, in both undoped and doped states, are tabulated in table 5.1. It was found that the undoped state of conventional PANI exhibited electrical conductivity in the order of 10^{-11} S/cm, confirming the insulating form (PANI EB). On the other hand, the electrical conductivity of conventional PANI in the doped state (PANI ES) was higher than

that of PANI EB, by approximately 12 orders of magnitude. This reflects the highly π-conjugated system and highly-ordered structure of PANI ES, consistent with the XRD results. Moreover, it was found that the overall conductivities of the synthesized dendritic PANI nanoparticles, in both undoped and doped states, were comparable to those prepared using the conventional method (King *et al.* 2005). Thus, this suggests that the resulting change in morphology does not significantly affect the electrical conductivity. Nevertheless, a word of caution must be added in that the electrical conductivities listed in table 5.1 were obtained from pressed pellets, and therefore the dendritic PANI nanoparticles may have experienced changes in morphology (when subjected to the pressure of the press) during the sample preparation. Therefore, the measured conductivities may in fact reflect a bulk polymer property.

Table 5.1 Electrical conductivity of polyaniline nanoparticle.

Sample*	Specific conductivity (S/cm)	
	Undoped state**	Doped state
PANI	$3.72 \times 10^{-11} \pm 9.86 \times 10^{-13}$	15.6 ± 0.32
PANI-(0.5CMCT)	$3.84 \times 10^{-11} \pm 9.48 \times 10^{-13}$	20.5 ± 0.90
PANI-(1CMCT)	$3.14 \times 10^{-11} \pm 1.23 \times 10^{-12}$	18.4 ± 0.99
PANI-(2CMCT)	$3.15 \times 10^{-11} \pm 1.17 \times 10^{-12}$	19.7 ± 1.37

* Sample was prepared by compression of polyaniline powder.

** The synthesized PANI ES powder was immersed in 1 M NaOH (1 g of PANI ES : 50 g of 1 M NaOH) for 2 h.

5.5 Conclusion

Uniform dendritic PANI nanoparticles with a narrow size distribution were successfully synthesized under acidic conditions in the presence of CM-chitin. It is proposed that the CM-chitin self-assembles to form a hydrophobic core that acts as a

template for monomer accumulation and subsequent polymerization. After the polymerization is completed, the CM-chitin template can be removed to obtain pristine dendritic PANI nanoparticles. The morphology of the dendritic PANI nanoparticles is globular, with radially-aligned PANI dendrites and with an average diameter in the nanometer range. The size of the dendritic PANI nanoparticles decreases with increase in the CM-chitin concentration. This seems likely due to a lower level of monomer uptake in each hydrophobic core, when the CM-chitin concentration is increased. Moreover, it was found that the addition of CM-chitin does not influence the crystal structure of the resulting PANI, and that the electrical conductivity of the pressed dendritic PANI nanoparticles is comparable to that of PANI synthesized without the CM-chitin template.

5.6 Acknowledgements

5.7 References

Bai, X. Li, X. Li, N. Zuo, Y. Wang, L. Li, J. and Qiu, S. (2007) Synthesis of cluster polyaniline nanorod via a binary oxidant system. Material Science and Engineering C, 27, 695-699.

Baxter, A. Dillon, M. and Taylor, K.D.A. (1992) Improved method for i.r. determination of the degree of N-acetylation of chitosan. International Journal of Biological Macromolecules, 14, 166-169.

Chan, H.S.O. Teo, M.T.B. Khor, E. and Lim, C.N. (1989) Thermal analysis of conducting polymers part I thermogravimetry of acid-doped polyanilines. Journal Thermal Analysis and Calorimetry, 35, 765–774.

Cheng, D. Ng, S. and Chan. H.S.O. (2005) Morphology of polyaniline nanoparticles synthesized in triblock copolymers micelles, Thin Solid Films. 477, 19-23.

Cho, M.S. Park, S.Y. Hwang, J.Y. and Cho, H.J. (2004) Synthesis and electrical properties of polymer composites with polyaniline nanoparticles. Materials Science and Engineering C, 24, 15-18.

Cruz-Silva, R. Romero-Garcia, J. Angulo-Sanchez, J.L. Ledezma-Perez, A. Arias-Matin, E. Moggio, I. and Flore-Loyola, E. (2005) Template-free enzymatic synthesis of electrically conducting polyaniline using soybean peroxidase. European Polymer Journal, 41, 1129-1135.

Ghanbari, K.H. Mousavi, M.F. and Shamsipur, M. (2006) Preparation of polyaniline nanofibers and their use as a cathode of aqueous rechargeable batteries. Electrochimica Acta, 52, 1514-1522.

He, Y. (2005) Preparation of polyaniline microspheres with nanostructured surfaces by a solids-stabilized emulsion. Material Letter. 59, 2133-2136.

Huang, J. and Kaner, R.B. (2004) A general chemical route to polyaniline nanofibers. Journal of the American Chemical Society, 126, 851-855.

Jang, J. Bae, J, and Lee, K. (2005) Synthesis and characterization of polyaniline nanorods as curing agent and nanofiller for epoxy matrix composite. Polymer, 46, 3677-3684.

Kan, J. Zhou, S. Zhang, Y. and Patel, M. (2006) Synthesis and characterization of polyaniline nanoparticles in the presence of magnetic field and samarium chloride. European Polymer Journal, 42, 2004-2012.

King, R.C.Y. and Roussel, F. (2005) Morphological and electrical characteristics of polyaniline nanofibers. Synthetic Metals, 153, 337-340.

Li, G. Pang, S. Xie, G. Wang, Z. Peng, H. and Zhang, Z. (2006) Synthesis of radially aligned polyaniline dendrites, Polymer, 47,1456-1459.

Li, M. Gou, Y. Wei, Y. MacDiarmid, A.G. Lelkes, P.I. (2006) Electrospinning polyaniline-contained gelatin nanofibers for tissue engineering applications. Biomaterials, 27, 2705-2715.

Li, X. Zhoa, Y. Zhuang, T. Wang, G. and Gu, Q. (2007) Self-dispersible conducting polyaniline nanofibres synthesized in the presence of β-cyclodextrin. Colloids and Surfaces A, 295, 146-151.

Low L.M. Seetharaman, S. He, K.Q. and Madou, M.J. (2000) Microactuators toward microvalves for responsive controlled drug delivery, Sensors and Actuators B, 67, 149-160.

Ma, X. Wang, M. Li, G. Chen, H. and Bai, R. (2006) Preparation of polyaniline–TiO_2 composite film with in situ polymerization approach and its gas-sensitivity at room temperature. Materials Chemistry and Physics, 98, 241-247.

Mi, F.L. Chen, C.T. Tseng, Y.C. Kuan, C.Y. and Shyu, S.S. (1997) Iron(III)-carboxymethylchitin microsphere for the pH-sensitive release of 6-mercaptopurine. Journal of Controlled Release, 44, 19-32.

Muramatsu, K. Masuda, S. Yoshihara, Y. and Fujisawa, A. (2003) In vitro degradation behavior of freeze-dried carboxymethyl-chitin sponges processed by vacuum-heating and gamma irradiation. Polymer Degradation and Stability, 81, 327-332.

Neoh, K.G. Kang, E.T. and Tan, K.L. (1990) Thermal degradation of leucoemeraldine, emeraldine base and their complexes. Thermochimica Acta, 171, 279–291.

Palma, R. Himmel, M.E. and Brady, J.W. (2000) Calculation of the Potential of Mean Force for the Binding of Glucose to Benzene in Aqueous Solution. Journal of Physical Chemistry B, 104, 7228–7234.

Pinto, N.J. Carrion, P.L. Ayala, A.M. and Ortiz-Marciale, M. (2005) Temperature dependence of the resistance of self-assembled polyaniline nanotubes doped with 2-acrylamido-2-methyl-1-propanesulfonic acid. Synthetic Metals, 148, 271-274.

Sahiner, N. (2007) Hydrogel nanonetworks with functional core–shell structure. European Polymer Journal, 43, 1709-1717.

Sawall, D.D. Villahermosa, R.M. Lipeles, R.A. and Hopkins, A.R. (2004) Interfacial polymerization of polyaniline nanofibers grafted to Au surfaces. Chemistry of Materials, 16, 1606-1608.

Sazou, D. Kourouzidou, M. and Pavlidou, E. (2007) Potentiodynamic and potentiostatic deposition of polyaniline on stainless steel: Electrochemical and structural studies for a potential application to corrosion control. Electrochimica Acta, 52, 4385-4397.

Shah, A.A. and Holze, R. (2006) Spectroelectrochemistry of aniline-*o*-aminophenol copolymers. Electrochimica Acta, 52, 1374-1382.

Stejskal, J. and Sapurina, I. (2004) On the origin of colloidal particles in the dispersion polymerization of aniline. Journal of Colloid and Interface Science, 274, 489-495.

Ueno, T. Yokota, S. Kitaoka, T. Wariishi, H. (2007) Conformational changes in single carboxymethylcellulose chains on a highly oriented pyrolytic graphite surface under different salt conditions. Carbohydrate Research, 342, 954-960.

Wang, C.Y. Mottaghitalab, V. Too, C.O. Spinks, G.M. and Wallace, G.G. (2007) Polyaniline and polyaniline–carbon nanotube composite fibres as battery materials in ionic liquid electrolyte. Journal of Power Sources, 163, 1105-1109.

Wongpanit, P. Sanchavanakit, N. Pavasant, P. Supaphol, P. Tokura, S. and Rujiravanit, R. (2005) Preparation and Characterization of Microwave-treated Carboxymethyl Chitin and Carboxymethyl Chitosan Films for Potential Use in Wound Care Application. Macromolecular Bioscience, 5, 1001-1012.

Xian, Y. Liu, F. Feng, L. Wu, F. Wang, L. and Jin, L. (2007) Nanoelectrode ensembles based on conductive polyaniline/poly(acrylic acid) using porous sol–gel films as template. Electro-chemistry Communications, 9: 773-780.

Xing, S. Zhao, C. Jing, S. and Wang, Z. (2006) Morphology and conductivity of polyaniline nanofibers prepared by 'seeding' polymerization, Polymer, 47, 2305-2313.

Xing, S. Zhao, C. Niu, L. Wu, Y. Wang, J. and Wang, Z. (2006) Diode-like behavior based on polyaniline and Pt. Solid-State Electronics, 50, 1629-1633.

Xiong, S. Wang, Q. and Xia, H. (2004) Preparation of polyaniline nanotubes array based on anodic aluminum oxide template. Material Research Bulletin, 39, 1569-1580.

Xiong, S. Wang, Q. and Xia, H. (2004) Template synthesis of polyaniline/TiO$_2$ bilayer microtubes. Synthetic Metals, 146, 37-42.

Yan, X.B. Han, Z.J. Yang, Y. Tay, B.K. (2007) NO$_2$ gas sensing with polyaniline nanofibers synthesized by a facile aqueous/organic interfacial polymerization. Sensors and Actuators B, 123, 107-113.

Yang, X. Zhao, T. Yu, Y. and Wei, Y. (2004) Synthesis of conductive polyaniline/epoxy resin composites: doping of the interpenetrating network. Synthetic Metals, 142, 57-61.

Yuan G, Kuramoto N, and Su S. (2002) Template synthesis of polyaniline in the presence of phosphomannan. Synthetic Metals, 129,173-178.

Zhang, D. and Wang. Y. (2006) Synthesis and applications of one-dimensional nano-structured polyaniline: An overview. Materials Science and Engineering B, 134, 9-19.

Zhang, X. Goux, W.J. and Manohar, S.K. (2004) Synthesis of polyaniline nanofibers by nanofiber seeding. Journal of the American Chemical Society. 126: 4502-4503.

Zhang, X. and Manohar, S.K. (2004) Bulk synthesis of polypyrrole nanofibers by a seeding approach. Journal of the American Chemical Society, 126, 12714-12715.